JOURNAL OF MATERIALS SCIENCE 30 (1995) 891–897

Laser processing to create *in-situ* Al-SiC_p surface metal matrix composites

C. HU, T. N. BAKER
Department of Metallurgy and Engineering Materials, University of Strathclyde, Glasgow G1 1XN, UK

When SiC particulate (SiC_p) is preplaced on an aluminium alloy surface, a molten zone can be formed in the aluminium specimen by laser processing, and there is a possibility of producing an *in-situ* Al-SiC_p metal matrix composite (MMC) layer on the surface, which will modify the surface properties. Under specific laser processing conditions in the present work, a smooth and continuous Al-SiC_p MMC layer was developed on the surface with well-distributed and embedded SiC_p in the layer. In most cases, the SiC_p partially dissolved in the liquid and reprecipitated during the solidification. The dissolution of the SiC_p is discussed, and the precipitate in the present work is identified as Al_4SiC_4. The thickness of the Al-SiC_p MMC layer was limited to 30–50 μm when SiC_p was preplaced on the specimen. The mechanism of both the formation of the Al-SiC_p and the limitation of the MMC layer thickness in this process was studied.

1. Introduction

Although high powered laser surface scanning has been utilized in steels [1–2], titanium alloys [3–4], and Stellite [5], the application of laser surface treatment to aluminium alloys has been limited because aluminium has an extremely low energy absorption from the laser beam, and also there is no significant phase transformation produced to give an observable modification of the surface during the process. However, aluminium is the most common alloy used as an MMC base alloy. The attractive physical and mechanical properties, such as high specific modulus and strength, which can be obtained with MMC materials, and thermal stability, have been extensively documented [6–12]. When the SiC_p, which has a high energy absorption from the laser, is preplaced on the surface of the aluminium alloy, and therefore the heat absorbed by the ceramic can be efficiently transferred to the surface, a molten zone may be produced, and an aluminium ceramic MMC layer on the surface may be produced under specific processing conditions. If the process is satisfactorily controlled, it will have the following two advantages: (1) it can be carried out on the surfaces of a component and avoid the difficulties in machining bulk MMC materials; and (2) it can be carried out on one, or a few of the faces of the component, such as a contact face, and therefore save time and energy.

Some initial experimental work has been carried out and showed promise. The results are presented and the influence of various process parameters on the microstructure produced by laser scanning, are discussed in this paper.

2. Experimental procedure

2.1. Materials

Commercially pure aluminium (CP-Al), 6061 and 8090 aluminium alloys were used as the base alloys. The compositions of the aluminium alloys are shown in Table I. SiC_p, 6.5 μm mean diameter, was used as the reinforced particulate preplaced on the alloy surface. The thickness of the preplaced layer was set at 30–50, 80–100, 130–150, and 190–210 μm, to follow the effect of the thickness. The base specimens have a thickness of 8 mm for all the experiments in the present work.

2.2. Processing

The SiC_p was blended with a binder, an organic solution, and painted on the surface prior to laser scanning. A stationary, continuous CO_2 laser beam was used, and the specimens were moved under the beam on a work-table to produce all the tracks processed in the present work. Argon gas was used at 50 l min^{-1} to protect the area glazed by the laser.

2.3. Processing Conditions

Three levels of q, the laser beam power, 2.8, 3.0 and 4.2 kW, four levels of r_B, the radius of the laser beam, 1, 1.5, 2 and 2.5 mm, and two levels of v, the velocity of the specimen, 5 and 15 mm s^{-1}, were used in the laser processing. Therefore the laser energy density $E = q/(r_B v)$ (MJ m^{-2}), referring to the energy intensity [1], is determined by q, r_B and v.

0022–2461

TABLE I. The compositions of the base alloys (wt %).

Base alloys	Fe	Si	Mg	Cu	Mn	Cr	Li	Zr	Ti	Zn	Al
Cp-Al	0.4	0.3	0.03	0.03	0.03	–	–	–	–	0.07	> 99.5
8090 alloy	0.15	0.1	0.95	1.3	0.05	0.05	2.45	0.1	0.05	0.13	extra
6061 alloy	0.21	0.7	1.02	0.27	0.04	0.2	–	–	–	–	extra

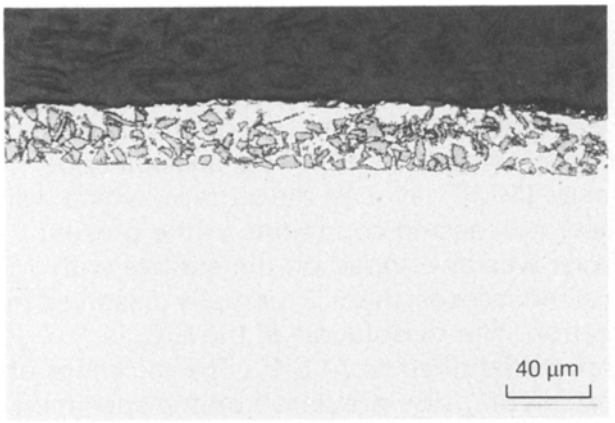

Figure 1 A micrograph in transverse section, of the MMC layer produced on CP-Al alloy surface, preplaced with SiC_p at a thickness of 35 μm, laser glazed at $q = 2.8$ kW, $r_B = 1$ mm, and $v = 5$ mm s^{-1}, $E = 0.56$ MJ m^{-2}.

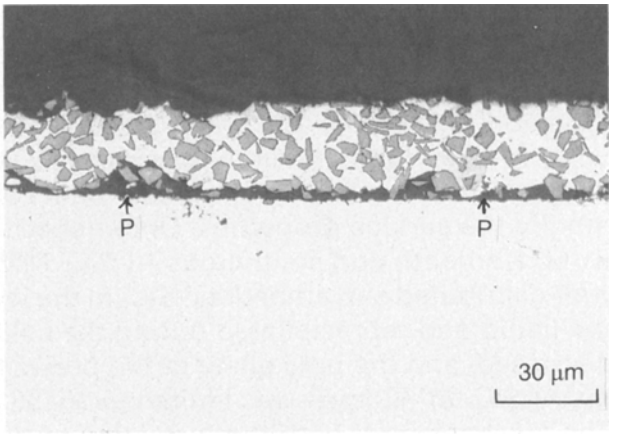

Figure 3 The micrograph in transverse section, of the same specimen as shown in Fig. 1, but taken at location 2, showing a smooth MMC layer and porosity between the layer and the base alloy.

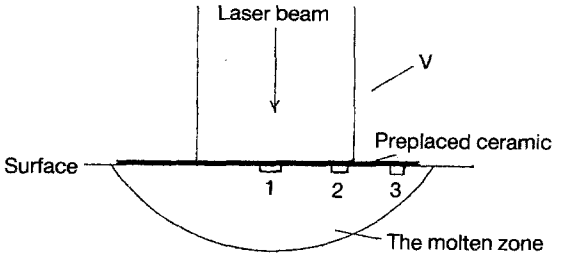

Figure 2 A schematic transverse section of base alloy, and the locations of the micrographs in Figs 3 and 4.

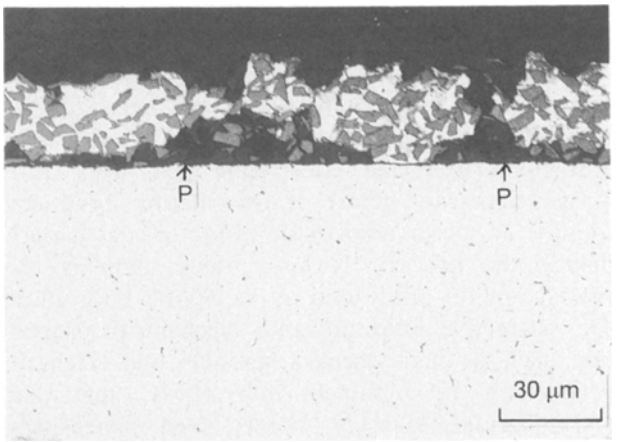

Figure 4 The micrograph in transverse section, of the same specimen as shown in Fig. 1, but taken at location 3, showing a discontinuous MMC layer and more porosity between the layer and the base alloy.

2.4. Examination

The laser treated microstructures were examined using an optical microscope and an SEM. A TEM and an associated Link EDX System were also used to identify the particles formed during the processing.

3. Results and Discussions

3.1. The incorporation of SiC_p at different locations

Under specific processing conditions, the SiC_p was well distributed in a smooth surface layer and well embedded in the matrix alloy of the MMC layer. This is shown in Fig. 1. The incorporation of the SiC_p depends also on the locations of the SiC_p, relative to the centre of the beam. For simplicity, a schematic diagram is given in Fig. 2 to show the locations mentioned in the following discussion. The micrograph in Fig. 1 was taken from location 1. Another micrograph taken from location 2 in the same specimen is shown in Fig. 3. In this case the layer is not smooth, and there is a significant degree of porosity (P) at the interface between the MMC layer and the base alloy matrix. The further the distance from the centre of laser beam, the less successful was the incorporation of the SiC_p on the surface in this particular specimen. A micrograph given in Fig. 4, taken at location 3, towards the edge of the molten zone, showed a discontinuous MMC layer, with extensive porosity at P between the layer and the base alloy.

Theoretically, for a given system of preplaced ceramic on the surface and base alloy, the incorporation of the ceramic requires a certain amount of liquid and a sufficient liquid lifetime during the process, which depend strongly on the temperature field generated in the process. During the laser processing there must be a very high temperature generated in the beam centre,

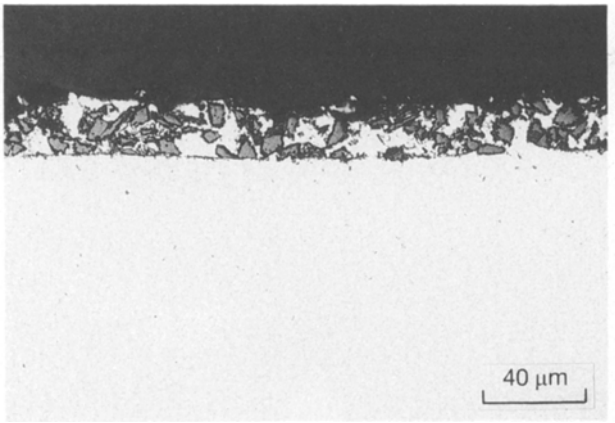

Figure 5 A micrograph in transverse section, of the MMC layer produced on 6061 Al alloy surface, preplaced with SiC_p at a thickness of 35 μm, laser glazed at $q = 2.8$ kW, $r_B = 1.5$ mm, and $v = 15$ mm s^{-1}, $E = 0.12$ MJ m^{-2}.

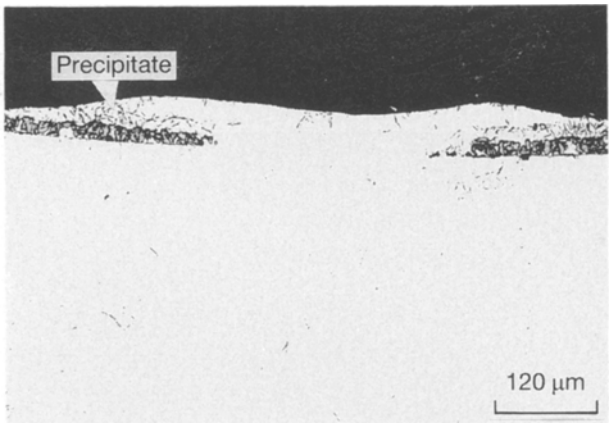

Figure 6 A microstructure in transverse section, produced on CP-Al alloy surface, preplaced with SiC_p at a thickness of 35 μm, laser glazed at $q = 4.2$ kW, $r_B = 1$ mm, and $v = 5$ mm s^{-1}, $E = 0.84$ MJ m^{-2}.

and the base alloy melting point must be exceeded at the edge of the molten zone. A low temperature near to the edges of molten zone produced a liquid of high viscosity [13] and a short lifetime, and therefore resulted in a poor incorporation of the SiC_p at a distance from the centre of the laser beam, a situation illustrated in Fig. 4.

3.2. The effect of laser processing conditions

When a low level of laser energy density $E = 0.12$ MJ m^{-2} ($q = 2.8$ kW, $r_B = 1.5$ mm, and v = 15 mm s^{-1}), was used, a poor incorporation of SiC_p could be also developed at location 1, as shown in Fig. 5. However, when the laser energy density was excessive, 0.84 MJ m^{-2} ($q = 4.2$ kW, $r_B = 1$ mm, and $v = 5$ mm s^{-1}), the MMC layer could be broken at the centre of the molten zone, and some resolidified particles formed in the melt pool, because the SiC particulates at the centre location were melted or dissolved. This is shown in Fig. 6, which also shows an uneven surface due to the influence of liquid surface tension

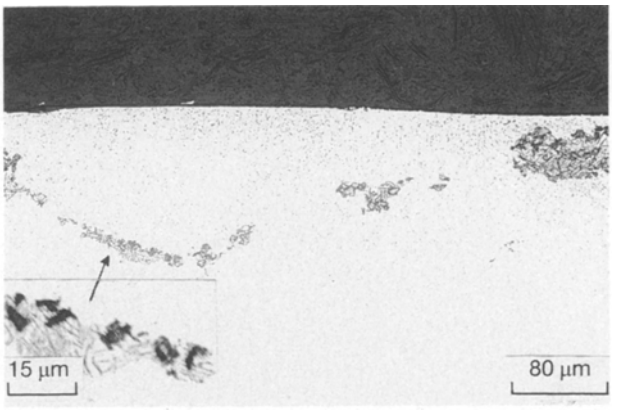

Figure 7 A microstructure in transverse section, produced on 8090 Al alloy surface, preplaced with SiC_p at a thickness of 35 μm, laser glazed at $q = 4.2$ kW, $r_B = 1$ mm, and $v = 15$ mm s^{-1}, $E = 0.28$ MJ m^{-2}, showing the SiC_p moved from the surface.

gradient, when an excessive level of laser energy density was developed.

3.3. The effect of a convective flow

A common phenomenon in the laser process is that there will be a convective flow generated in the liquid, due to a steep surface tension gradient in the liquid [14, 15]. When the convective flow is small and/or slow, its effect on the incorporation of SiC_p is negligible, which might be advantageous. When the convective flow is strong, it will cause a movement of the SiC_p from the surface into the liquid pool. This is shown in Fig. 7, which was taken from location 1, as defined in Fig. 2, and shows that the MMC layer was broken up, and the SiC_p at the centre was moved down into the liquid below the surface. The profile of the solid SiC_p distributed in the microstructure has a shape of a discontinuous "v". It is thought that a scanning direction symmetrically distributed laser energy will cause a symmetric temperature field, and a convective flow in the liquid. Therefore, it can be considered that a strong convective flow may cause a movement of SiC_p from the molten surface, and result in the discontinuous "v"-shaped SiC_p distribution profile, seen in transverse sections

3.4. SiC_p dissolution and precipitation

Fig. 6 shows that particles were found in the molten zone and have the shape of needles. The micrograph in Fig. 7 shows some particles formed near to the SiC_p, which itself has a small size, moved down from the surface into the liquid. In addition, it is also noticed from Fig. 7 that the quantity of the SiC_p which moved down into the liquid and the particles nearby, together have a volume fraction much less than that of the original SiC_p. This suggests that SiC_p partially dissolved into the liquid during the processing, and particles were formed during solidification.

Typical SEM and TEM micrographs of the particle are given in Figs 8 and 9 respectively. The particle has a needle structure, is thin and long, and distributed in the matrix. An EDX spectrum (Fig. 10) imaged in a foil

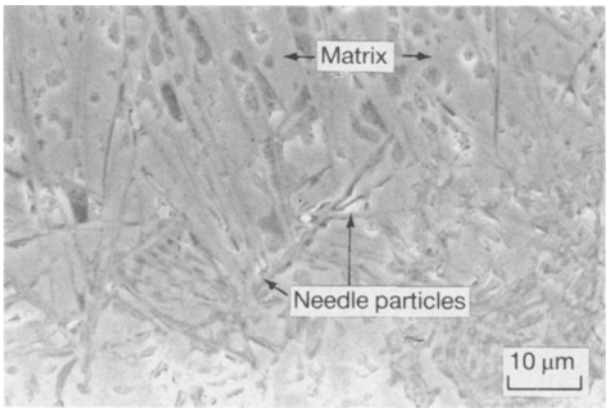

Figure 8 A SEM micrograph in transverse section, of the particle formed during the laser process, showing a finely branched and needle shaped particle microstructure.

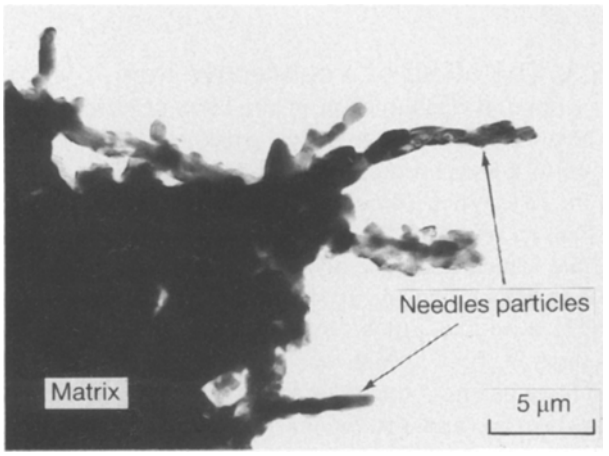

Figure 9 A TEM micrograph of the particle.

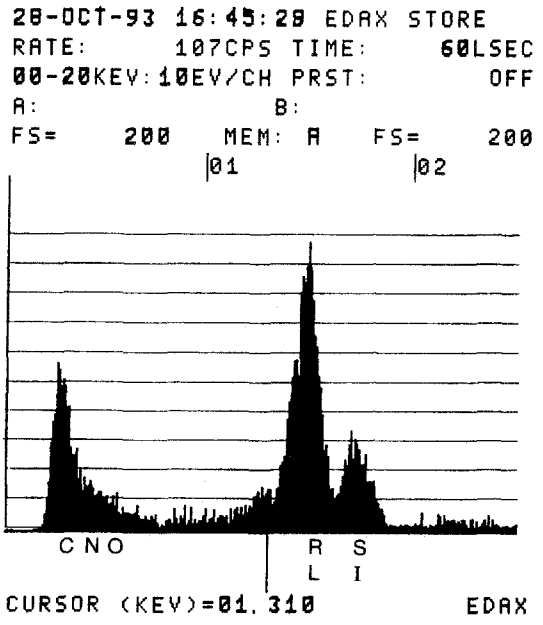

Figure 10 The EDX spectrum from the particle as shown in Fig. 9.

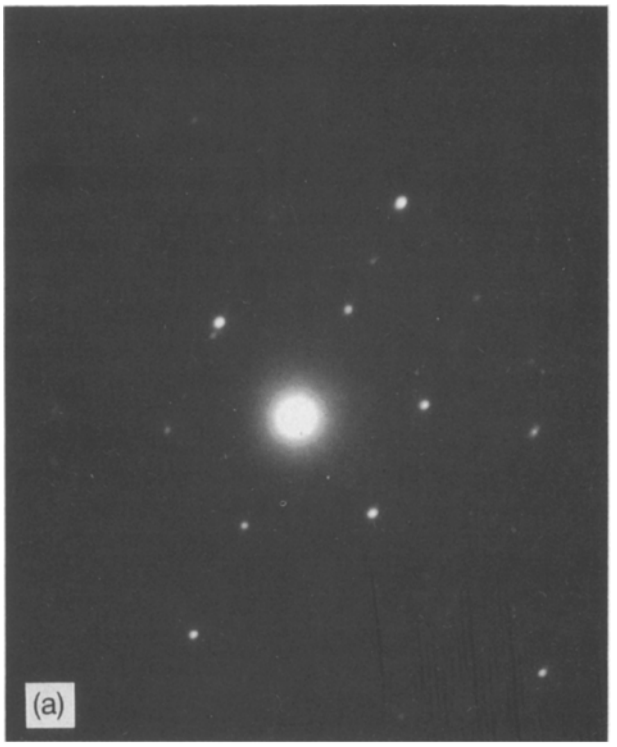

Figure 11 The electron diffraction patterns from the compound: (a) and (b) were obtained from the same phase at different angles.

specimen from the particle, shows carbon, aluminium and silicon. The energy dispersive spectroscopy (EDX) from the matrix (not illustrated) does not show any carbon, but a much lower level of silicon, which suggests that the particle must be a compound of silicon and carbon, and contains more carbon atoms than silicon atoms. Two electron diffraction patterns from the compound, at different orientations, are given in Figs. 11(a) and (b). An electron diffraction pattern of the aluminium matrix, assumed to be a pure

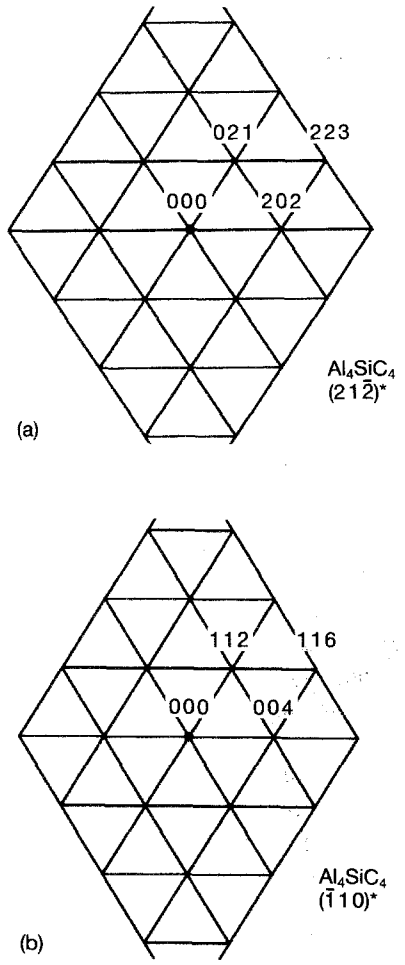

Figure 12 The schematic diffraction patterns (a) and (b) for Figs. 11a and b respectively.

aluminium matrix, was used to determine the camera constant, and therefore, allow the identification of the compound. The schematic interpretation of the electron diffraction patterns in Figs. 11(a) and (b) is given in Figs. 12(a) and (b) respectively. As a result of the identification, the compound is considered to be Al_4SiC_4 and formed from the reaction

$$4Al + 4SiC = Al_4SiC_4 + 3Si \quad (1)$$

Al_4SiC_4 has a hexagonal crystal structure with $a = 5.65$ Å and $c = 10.8$ Å [16]. The calculated and measured d and θ values (based on $a = 5.65$ and $c = 10.8$ Å) are given in Table II. The possibility of the needles being Al_4C_3 (hexagonal, $a = 3.331$ Å and $c = 24.99$ Å [16]) has been considered, but it has not been found possible to index the cross-grating patterns obtained in this work based on this compound. Therefore the EDX spectrum together with the selected area electron diffraction (SAED) patterns strongly suggest that the needles are Al_4SiC_4. From Equation 1, it is also indicated that when one molecule of Al_4SiC_4 is formed, there will be three atoms of silicon dissolved into the solid solution of the alloy matrix. This is in a good agreement with all the EDX spectra. Equation 1 also suggests that the dissolution of SiC_p in the liquid will affect the formation of new compounds. Furthermore, a high solubility and diffusivity of the silicon, and a low silicon content in the base alloy, will promote the SiC_p dissolution into the base alloy, and therefore have an effect on precipitation. Additionally, a convective flow generated in the molten zone will promote the SiC_p dissolution by increasing the silicon concentration gradient, and consequently the silicon diffusion rate in the liquid surrounding the SiC_p.

Several studies have addressed the problem of identification of the interface layers which have been observed when SiC reacts with aluminium and its alloys. T. Iseki *et al.* [17] studied the reactions between SiC and liquid aluminium. TEM showed that aluminium carbide, Al_4C_3 was formed at the interface between pressureless sintered SiC and aluminium. Kannikesweran and Liu [18] addressed the same problem, and examined the SiC-Al interface in a 1100 aluminium alloy using SEM-EDX. This technique did not prove sufficiently sensitive to allow identification of individual compounds in the reaction layer. In another example it has been shown that, in heat-treated Al-Mg/SiC composites, a very thin layer of reaction product Al_4C_3 compounds occurs, which appears to inhibit interfacial sliding and apparently increased the elastic modulus [19]. The reaction product follows from the equation used by Iseki *et al.* [17]

$$4Al + 3SiC = Al_4C_3 + 3Si \quad (2)$$

which was also proposed to be responsible for the observations of Johnson *et al.* [20], who examined the interface resulting from the reaction between SiC_p and liquid Al, and between 13 μm SiC_p and liquid Al-12 wt% Si. Their TEM results, from a rapidly quenched matrix liquid state, showed that Al_4C_3 nucleated at heterogeneous sites of preferred SiC dissolution. Al_4C_3 was not found in a 6061 SiC_p composite, manufactured by liquid-phase sintering with 63 μm particulate [21], but the SiC-matrix interfaces were found to have various degrees of faceting, an observation considered to be due to the locally

TABLE II. Some related Al_4SiC_4 crystal structure data.

hkl	d (Å) based on [16]	d (Å) measured	θ ($h_1k_1l_1$, $h_2k_2l_2$) calculated	θ ($h_1k_1l_1$, $h_2k_2l_2$) measured
112	2.803	2.81	56.88° (021, 202)	57° (021, 202)
004	2.700	2.69	29.82° (021, 223)	30° (021, 223)
116	1.578	1.59	27.06° (202, 223)	27° (202, 223)
021	2.747	2.75	58.72° (112, 004)	59° (112, 004)
202	2.514	2.55	29.97° (112, 116)	30° (112, 116)
223	1.492	1.52	28.80° (004, 116)	29° (004, 116)

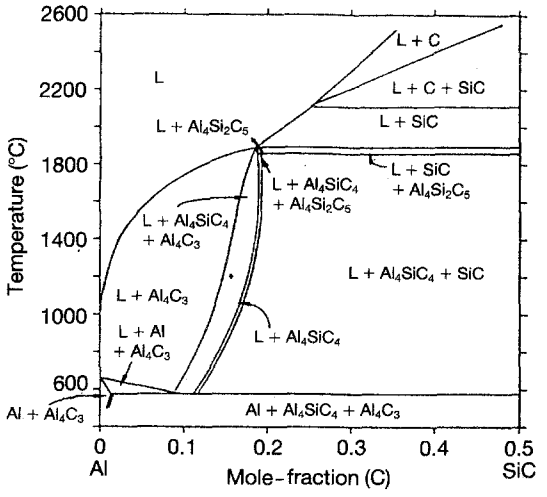

Figure 13 The Al-SiC isopleth for the temperature range 400 to 2600 °C [22].

high concentrations of alloying elements, which occur during sintering.

Although most of the previous work mentioned above favoured the hypothesis that the precipitation of Al_4C_3 occurred from the reaction between SiC_p and liquid Al in bulk MMC samples, Lee *et al.* [22] indicated that both the Al_4C_3 and Al_4SiC_4 could be formed, depending on the SiC concentration in the liquid. Fig. 13 shows a corner of Al-SiC isopleth which indicates that when the SiC content in the liquid exceeds 20% mole fraction, Al_4SiC_4 will be formed from the liquid. In the laser processing, the formation of liquid, the SiC_p dissolution, the formation of new compounds, and the solidification of the melt, all occur in a very short time, which restricts the diffusion in the liquid, and results in a high silicon and carbon content near the SiC_p. Therefore Al_4SiC_4 is formed in preference to Al_4C_3 as seen in Figs 7 and 8. The convective flow may move Al_4SiC_3 away from SiC_p but the very short lifetime of the liquid does not allow other reactions or phase transformations to occur.

However, some surface properties such as wear resistance, require solid SiC_p to remain after the laser scanning. This situation may be obtained by using a low solubility ceramic in the associated base alloy system and/or controlling the temperature field and convective flow in the process.

3.5. The thickness of the preplaced SiC_p

The thickness of an Al-SiC_p MMC layer, which could be successfully produced in this laser process, was up to 50 μm. Increasing the thickness of preplaced SiC_p further did not give the expected microstructure. When a thicker SiC_p layer was preplaced on the surface, an MMC layer could be also obtained on the surface with the SiC_p well distributed, but the layer was separated from the base alloy by a large cavity generated in the molten zone. The greater the preplaced SiC_p thickness, the larger the cavity. This suggests that the formation of an Al-SiC_p MMC layer requires a sufficient volume of liquid filling into the preplaced SiC_p layer. The liquid comes only from the molten zone produced underneath the laser beam, with a restricted liquid volume. In the case of a thick preplaced SiC_p layer, a large volume of liquid is needed from the restricted source, and eventually a large cavity remains after the laser glazing. In addition to the cavities, the MMC layer was poorly incorporated with the alloy surface on the other areas. This implies that the liquid in the molten zone infiltrated into the preplaced SiC_p layer through the centre of the liquid surface, and then spread within the layer, towards both sides. Therefore, a mechanism is suggested in which the capillary force drags the liquid upwards to fill the porosity in the preplaced layer. The liquid has the highest temperature and lowest viscosity at the centre of its surface, and therefore it is here that it has its highest potential capillarity. The convective flow due to a high surface tension gradient in the liquid may promote this liquid movement, because of the same direction of the liquid flow. Therefore, it is suggested that the energy distribution of the laser processing determines the thickness limit of using preplaced SiC_p and the formation of cavities if the preplaced SiC_p thickness limit is exceeded.

The thickness of the preplaced SiC_p layer is also thought to affect the temperature field, and therefore affect the size and shape of the molten zone, because energy is only absorbed on the surface, and the preplaced SiC_p layer behaves as an insulating medium during the energy transfer from the surface to the base alloy. Qualitatively, the energy transferred into the base alloy will be decreased and so will the temperature and the molten zone, when the preplaced SiC_p layer is thick.

4. Summary

The formation of an Al-SiC_p MMC layer requires a critical laser energy density to be exceeded to provide a suitable temperature in the process. Under specific processing conditions, a smooth Al-SiC_p MMC layer can be produced at the centre of the molten zone surface with well distributed and embedded SiC_p in the layer. The liquid filling into the preplaced SiC_p layer is driven mainly by the capillary action. The convective flow generated in the liquid during the process has an important influence on the distribution and the dissolution of the SiC_p in the processed microstructures. A strong convective flow can move SiC particulates down into the liquid pool.

A compound, which is needle shaped and finely branched, was formed in the matrix during the laser processing. It was identified by SAED and EDX as Al_4SiC_4 and considered to be formed by the reaction $3Al + SiC_p = Al_4SiC_4 + 3Si$. The excess silicon from the reaction remained in solid solution in the aluminium matrix. The thickness of the preplaced SiC_p was limited to about 50 μm for the present laser processing conditions, due to the development of a cavity below the subsequently formed MMC layer which was brittle, and fractured and collapsed into the cavity during metallographic preparation.

Acknowledgements

The authors wish to thank DTI/MOD/RAE for the financial support and Professor A.W. Bowan and Dr Ubhi at RAE for helpful discussions. Alcan are thanked for supplying the aluminium alloys.

References

1. M. F. ASHBY and K. E. EASTERLING *Acta Metall.* **32** (1984) 1935.
2. A. SCHÜSSLER, P. H. STEEN and P. EHRARD, *Appl. Phys.* **71** (1992) 1972.
3. S. MRIDHA and T. N. BAKER, *Mater. Sci. Eng.* **A142** (1991) 115.
4. K. P. COOPER and J. D. AYERS, *Surface Eng.* **1** (1985) 263.
5. G. ABBAS and D. R. F. WEST, *Wear* **143** (1991) 353.
6. S. G. FISHMAN, *J. Met.* **38** (1986) 36.
7. *Idem., Mater. Sci., Eng.* **77** (1986) 181.
8. A. H. M. HOWES, *J. Met.* **38** (1986) 28.
9. A. MORTENSEN, M. N. GUNGOR, J. A. CORNIE and M. C. FLEMINGS, *J. Met.* **40** (1988) 12.
10. A. MORTENSEN, J. A. CORNIE and M. C. FLEMINGS, *J. Met* **38** (1986) 30.
11. V. C. NARDONE and K. W. PREWO, *Scripta. Metall.* **20** (1986) 43.
12. A. IBRAHIM, F. A. MOHAMEDAND and E. J. LAVERNIA, *J. Mater. Sci* **26** (1991) 1137.
13. I. EGRY, *Scripta Metall. Mater.* **28** (1993) 1273.
14. T. R. ANTHONY and H. E. CLINE, *J. Appl. Phys.* **48** (1977) 3888.
15. C. CHAN, J. MAZUMDER and M. M. CHEN, *Metall. Trans., A* (15A) 1984 2175.
16. S. WEISSMANN *et al.* (eds),"Selected Powder Diffraction Data for Metals and Alloys" (first edition, JCPDS, USA, 1978), p. 689.
17. T. ISEKI, T. KAMEDA and T. MARRAUYAMA, *J. Mat. Sci.* **19** (1984) 1692.
18. K. KANNIKESWAREN and R. LIU, *J. Met.* **39** (1987) 17.
19. T. J. WARNER and W. M. STOBBS, in Proceedings of the 7th International Conference on Comp Mat (ICCM7), edited by W. Yunshu, G. Zhenlong and Renjie (Pergamon, New Work, 1989), p. 503.
20. P. K. JOHNSON, H. M. FLOWER and D. R. F WEST, in Conference Excluded Abstracts, Metal Matrix Composites–Property Optimisation and Applications, Institute of Metals, 1989, p 16.1.
21. G. M. JANOOWSKI and B. J. PLETKA, *Mat. Sci. Eng.* **A129** (1990) 65.
22. DOH-JAE LEE, M. D. VAUDIN, C. A. HANDWERKER and U. R. KATTNER, *Mater. Res. Symp. Proc.* **120** (1988) 293.

Received 7 January 1994
and accepted 28 June 1994